Propagators in Lagrangian space

Francis Bernardeau
Service de Physique Théorique, CEA/DSM/SPhT,
Unité de recherche associée au CNRS, CEA/Saclay, 91191 Gif-sur-Yvette cédex and
Canadian Institute for Theoretical Astrophysics, University of Toronto,
60 St. George street, Toronto, Ontario M5S 3H8, Canada

Patrick Valageas
Service de Physique Théorique, CEA/DSM/SPhT,
Unité de recherche associée au CNRS, CEA/Saclay, 91191 Gif-sur-Yvette cédex
(Dated: May 6, 2008)

It has been found recently that propagators, e.g. the cross-correlation spectra of the cosmic fields with the initial density field, decay exponentially at large-k in an Eulerian description of the dynamics. We explore here similar quantities defined for a Lagrangian space description. We find that propagators in Lagrangian space do not exhibit the same properties: they are found not to be monotonic functions of time, and to track back the linear growth rate at late time (but with a renormalized amplitude). These results have been obtained with a novel method which we describe alongside. It allows the formal resummation of the same set of diagrams as those that led to the known results in Eulerian space. We provide a tentative explanation for the marked differences seen between the Eulerian and the Lagrangian cases, and we point out the role played by the vorticity degrees of freedom that are specific to the Lagrangian formalism. This provides us with new insights into the late-time behavior of the propagators.

PACS numbers: 98.80.-k, 98.80.Bp, 98.65.-r

I. INTRODUCTION

Although the details of the evolution of the large-scale structure of the universe are probably affected by the presence of baryonic matter, in the context of a dark matter dominated cosmic fluid, it is thought that the global properties of the matter distribution at cosmological scales are essentially determined by those of a self-gravitating dust fluid.

A complete understanding of the development of gravitational instabilities in such a fluid is still however an open problem. It is one of the central issues for the study of structure formation in observational cosmology and this is for instance what pure N-body cosmological simulations attempt to solve. The Vlasov equation, that is the fluid limit of the Boltzmann equation, entirely describes this system (see [1] or [2] for details). This equation of motion applies to the so-called Eulerian description of the dynamics, where the fluid properties are described through functions of fixed space-time coordinates (such as density and velocity fields). However, there exists an alternative description where the system is defined by the trajectories of particles, labelled as a function of their initial positions. This is the Lagrangian formalism, which takes advantage of the particle description of the fluid. While this may not be a convenient description of the dynamics in the fully developed non-linear regime, it gives good insights of the dynamics in the early stages of the development of the gravitational clustering. The widely used Zel'dovich approximation [3] corresponds for instance to a description of the displacement field based on its linear approximation.

There exists a standard perturbative approach to study the development of gravitational instabilities beyond the linear approximation. This approach, and the main results it led to, is described to a large extent in [2]. While it can can be useful for some specific observables, it fails to provide effective tools for describing the evolution of quantities such as the density power spectrum beyond the linear regime. Then, one still needs to use semi-analytic prescriptions. The ones that are mostly used now, e.g. the so-called Peacock and Dodds formula [4] or the Smith et al. formula [5], originate either from the near universal transform advocated in [6], or are based on an even more empirical construction, the halo model (see [7]). It is to be noted though that these prescriptions offer predictions for the power spectrum with relatively low accuracy, at the level of 10%, and are insecure in cases of non standard cosmological models. Clearly there is a need to do better!

Recently there has been a revival of Perturbation Theory techniques (see [8, 9, 10, 11] and also [12] for an overview of these ideas). In particular the Renormalized Perturbation Theory (hereafter RPT) formalism introduced in [8] suggests a new scheme for the construction of perturbation theory expansions. It has been successfully applied to the shape of the two-point propagator, [13], and consequently to the two-point density power spectrum [14]. One of the core objects of this approach are the so-called propagators. They can be viewed as the cross-correlation between the cosmic fluids (that can either be the local density contrast or the peculiar velocity divergence) and the initial density field. In particular, it has been found that these correlators decay exponentially in the large-k limit (where k is the Fourier mode of interest). This result has been obtained analytically from a partial resummation of diagrams - in a perturbation theory point of view - that are thought to be the leading contributors of the high-k behavior of this quantity. It has been furthermore confirmed in numerical simulations.

The aim of this paper is to consider similar quantities in the Lagrangian description of the dynamics. Thus, our goal is not to reconstruct the real space power spectrum from Lagrangian variables (as done in [15]) but to extend, to other objects of interest that arise in the Lagrangian framework, exact PT results. We first recall in section II the basic ingredients of this description. To compute the high-k limit of the propagators we then assume Gaussian initial conditions and that the same set of diagrams will provide us with the leading contributions. To be more specific, those diagrams are those in which all loops are connected to the principal line. As shown in [16], and explained in details here, this approximation amounts to linearize the motion equation for a mode evolution while the low-k modes act as a random stochastic background. As we show in section III for the 2D dynamics and in section IV for the 3D, although the modes of this stochastic background - assumed to be of Gaussian statistics - are in infinite number, their effects can be recast as those of a finite number of Gaussian random variables. This method reveals extremely powerful. We explicitly show the results it leads to for the 2D and 3D-Lagrangian propagators. We summarize in the last section what we have learned from these calculations.

II. LAGRANGIAN APPROACH

A. Equations of motion

In Lagrangian approaches the global properties of the fluid are reconstructed from the individual particle trajectories, $\mathbf{x}(\mathbf{q},t)$, labeled by their initial Lagrangian coordinate $\mathbf{q}$. Thus, the Eulerian comoving position $\mathbf{x}$ at time t reads as

$$\mathbf{x} = \mathbf{q} + \Psi(\mathbf{q},t), \tag{1}$$

where $\Psi(\mathbf{q},t)$ is the displacement field. Note that in Eq.(1) we use the property that in standard cosmological scenarios the cold dark matter has a negligible initial velocity dispersion (as opposed to “hot” dark matter scenarios). This allows us to fully define the particles by their initial Lagrangian coordinate $\mathbf{q}$ with a unique initial peculiar velocity $\mathbf{v}(\mathbf{q})$. Then, the equation of motion for each particle reads as, once the homogeneous expansion of the Universe has been taken into account,

$$\frac{\partial^2 \mathbf{x}(\mathbf{q})}{\partial \tau^2} + \mathcal{H}\frac{\partial \mathbf{x}(\mathbf{q})}{\partial \tau} = -\nabla_{\mathbf{x}}\phi(\mathbf{q}), \tag{2}$$

where $\tau = \int \mathrm{d}t/a$ is the conformal time (and a the scale factor) and $\mathcal{H} = \mathrm{d}\ln a/\mathrm{d}\tau$ the conformal expansion rate. The gravitational potential ϕ is given by Poisson's equation

$$\Delta_{\mathbf{x}}\phi = \frac{3}{2}\Omega_{\mathrm{m}}\mathcal{H}^2\delta(\mathbf{q}), \tag{3}$$

where Ω_{m} is the matter density cosmological parameter and $\delta(\mathbf{q}) = (\rho-\overline{\rho})/\overline{\rho}$ the matter density contrast. It is to be noted that in this expression the Laplacian is taken with respect to the $\mathbf{x}$ coordinates while the fields are naturally given as a function of $\mathbf{q}$ through the expression of the displacement field. We assume here that the density contrasts vanish at initial time. The conservation of matter then implies that

$$1+\delta(\mathbf{q}) = \frac{1}{J(\mathbf{q})} \quad \text{with} \quad J(\mathbf{q}) = \left|\det\left(\frac{\partial \mathbf{x}}{\partial \mathbf{q}}\right)\right|. \tag{4}$$

Then, by taking the divergence with respect to the Eulerian coordinate $\mathbf{x}$ of the equation of motion (2) we obtain

$$J(\mathbf{q})\,\nabla_{\mathbf{x}}.\left[\frac{\partial^2\Psi(\mathbf{q})}{\partial\tau^2} + \mathcal{H}\frac{\partial\Psi(\mathbf{q})}{\partial\tau}\right] = \frac{3}{2}\Omega_{\mathrm{m}}\mathcal{H}^2(J(\mathbf{q})-1) \tag{5}$$

where we used Poisson's equation. As in the Eulerian case, it is convenient to introduce the time coordinate η and the function $f(\tau)$ defined from the linear growth rate $D_+(\tau)$ as,

$$\eta = \ln D_+(\tau), \quad f = \frac{\mathrm{d}\ln D_+}{\mathrm{d}\ln a} = \frac{\mathrm{d}\ln D_+}{\mathcal{H}\mathrm{d}\tau}. \tag{6}$$

The linear growth rate $D_+(\tau)$ is the growing solution of

$$\frac{\mathrm{d}^2 D_+}{\mathrm{d}\tau^2} + \mathcal{H}\frac{\mathrm{d}D_+}{\mathrm{d}\tau} = \frac{3}{2}\Omega_{\mathrm{m}}\mathcal{H}^2 D_+, \tag{7}$$

which we normalize as $D_{+0} = 1$ today. Then, Eq.(5) reads as

$$J(\mathbf{q})\,\nabla_{\mathbf{x}}.\left[\Psi''(\mathbf{q}) + \left(\frac{3\Omega_{\mathrm{m}}}{2f^2}-1\right)\Psi'(\mathbf{q})\right] = \frac{3\Omega_{\mathrm{m}}}{2f^2}(J(\mathbf{q})-1) \tag{8}$$

where we note with a prime the partial derivative with respect to time η.

In the following we will restrict the calculations to the Einstein-de Sitter case for which $\Omega_{\mathrm{m}}/f^2 = 1$. It is to be noted however that for all models of cosmological interest we have $\Omega_{\mathrm{m}}/f^2 \simeq 1$ so that this assumption is very mildly restrictive [2]. Thus, up to a good approximation, our results can be extended to ΛCDM cosmologies by substituting for the appropriate linear growth rate $D_+(\tau)$. Then, the dependence on the cosmological parameters is fully contained in the time-redshift relation $\eta(z)$.

Equation (8) can be written in matrix form as

$$\mathrm{Tr}\left[\left(\mathrm{com}(\frac{\partial \mathbf{x}}{\partial \mathbf{q}})\right)^T.\left(\frac{\partial \Psi''}{\partial \mathbf{q}} + \frac{1}{2}\frac{\partial \Psi'}{\partial \mathbf{q}}\right)\right] = \frac{3}{2}(J(\mathbf{q})-1), \tag{9}$$

where $\mathrm{com}(\frac{\partial \mathbf{x}}{\partial \mathbf{q}})$ is the comatrix of $(\partial \mathbf{x}/\partial \mathbf{q})$. It is also given by:

$$\left(\frac{\partial \mathbf{q}}{\partial \mathbf{x}}\right) = \left(\frac{\partial \mathbf{x}}{\partial \mathbf{q}}\right)^{-1} = \left(\mathrm{com}(\frac{\partial \mathbf{x}}{\partial \mathbf{q}})\right)^{T} / \det(\frac{\partial \mathbf{x}}{\partial \mathbf{q}}). \tag{10}$$

Thus, Eq.(9) is the form of the equation of motion (2) written in terms of the Lagrangian displacement field Ψ alone. However, it is not sufficient to fully determine the dynamics as can be noticed from the fact that we only used the potential part of Eq.(2) when we took the divergence in Eq.(5). Thus, we must supplement Eq.(9) with the rotational part:

$$\nabla_{\mathbf{x}} \times \left[\frac{\partial^2 \Psi(\mathbf{q})}{\partial \tau^2} + \mathcal{H} \frac{\partial \Psi(\mathbf{q})}{\partial \tau}\right] = 0. \tag{11}$$

As is well-known from the Eulerian perturbation theory, the rotational part of the Eulerian peculiar velocity field $\mathbf{v}$ decays in the linear regime and a curl-free initial velocity field remains potential to any order in perturbation theory [1, 2] (but vorticity will be generated by shell-crossings, see [17] for an estimation of this effect). Then, one usually restricts the dynamics to the case of irrotational initial velocity fields, $\nabla_{\mathbf{x}} \times \mathbf{v} = 0$, so that Eq.(11) simplifies to:

$$\nabla_{\mathbf{x}} \times \Psi'(\mathbf{q}) = 0, \quad \text{hence} \quad \frac{\partial \Psi'_i(\mathbf{q})}{\partial x_j} = \frac{\partial \Psi'_j(\mathbf{q})}{\partial x_i}, \tag{12}$$

which is of first order over time. In matrix form this constraint implies that [18],

$$\left(\frac{\partial \Psi'(\mathbf{q})}{\partial \mathbf{q}}\right) . \left(\mathrm{com}(\frac{\partial \mathbf{x}}{\partial \mathbf{q}})\right)^{T} \quad \text{is a symmetric matrix.} \tag{13}$$

In three-dimensional space Eqs.(13) are cubic in Ψ and Ψ' (in general they are of the order of the number of space dimensions). However, it is possible to derive equivalent equations that are quadratic in Ψ whatever the dimensionality of space. They can be obtained through the introduction of the velocity potential, Υ, which the velocity field is assumed to derive from, $\psi'_i(\mathbf{q}) \equiv \partial \Upsilon / \partial x_i$, in $\mathbf{x}$ coordinates. Expressing Υ in term of Ψ and imposing that $\partial^2 \Upsilon / \partial q_i \partial q_j$ is symmetric leads to an equivalent set of equations of lower order in ψ, [19]. These equations can also be derived explicitly from Eq.(12) by multiplying it by $(\partial x_i / \partial q_m)(\partial x_j / \partial q_\ell)$,

$$\frac{\partial x_i}{\partial q_m} \frac{\partial \Psi'_i(\mathbf{q})}{\partial q_\ell} = \frac{\partial x_j}{\partial q_\ell} \frac{\partial \Psi'_j(\mathbf{q})}{\partial q_m}, \tag{14}$$

a constraint that in matrix form states that,

$$\left(\frac{\partial \mathbf{x}}{\partial \mathbf{q}}\right)^{T} . \left(\frac{\partial \Psi'(\mathbf{q})}{\partial \mathbf{q}}\right) \quad \text{is a symmetric matrix.} \tag{15}$$

Equations (14)-(15) are quadratic over Ψ hence they are more convenient to use than Eqs.(12)-(13) in three (or more) dimensions [21].

B. Linear regime

The first stages of the dynamics take place at a time when the deviations from the Hubble flow are small. Then, the equations of motion can be linearized over the displacement field Ψ. From Eq.(4) the Jacobian $J(\mathbf{q})$ then reads up to linear order,

$$J_L(\mathbf{q}) = 1 + \mathrm{Tr}\left(\frac{\partial \Psi_L(\mathbf{q})}{\partial \mathbf{q}}\right) = 1 + \sum_i \Psi_{Li,i} = 1 - \kappa_L, \tag{16}$$

where we note with a subscript L all linear quantities. Note also that hereafter we define $\Psi_{i,j}$ as the partial derivative of the displacement field with respect to Lagrangian coordinates,

$$\Psi_{i,j}(\mathbf{q}) = \frac{\partial \Psi_i}{\partial q_j}, \tag{17}$$

and we introduced its divergence $-\kappa$,

$$\kappa(\mathbf{q}) = -\nabla_{\mathbf{q}}.\Psi(\mathbf{q}) = -\sum_i \frac{\partial \Psi_i(\mathbf{q})}{\partial q_i}. \tag{18}$$

It is to be noted that at linear order κ is nothing but the density contrast. Its time derivative is proportional to the velocity divergence. The motion equation (9) naturally reads at linear order,

$$\kappa''_L(\mathbf{q}) + \frac{1}{2}\kappa'_L(\mathbf{q}) = \frac{3}{2}\kappa_L(\mathbf{q}), \tag{19}$$

where we recover the two well-known growing and decaying linear modes:

$$\kappa_+ = e^{\eta} \quad \text{and} \quad \kappa_- = e^{-3\eta/2}. \tag{20}$$

In the following, we shall assume that the initial conditions are such that only the linear growing mode is present (but it would be possible to set different initial conditions):

$$\kappa_L(\mathbf{q}, \eta) = e^{\eta} \kappa_0(\mathbf{q}) \quad \text{hence} \quad \delta_L(\mathbf{q}, \eta) = e^{\eta} \kappa_0(\mathbf{q}). \tag{21}$$

Note then that at this order the constraint, Eq.(13), implies that $\Psi'_L(\mathbf{q})$ is curl-free in $\mathbf{q}$ coordinates, $\nabla_{\mathbf{q}} \times \Psi'_L(\mathbf{q}) = 0$, and so is the linear displacement field. It is then entirely determined by its divergence κ.

C. Correlators and propagators

Because of the mathematical structure of the theory, it is obviously very convenient to rewrite the motion equations in Fourier space. The Fourier components of the field are defined as,

$$\kappa(\mathbf{k}) = \int \frac{\mathrm{d}^n \mathbf{q}}{(2\pi)^n} e^{-\mathrm{i}\mathbf{k}.\mathbf{q}} \kappa(\mathbf{q}), \tag{22}$$

where $\mathrm{d}^n\mathbf{q}$ is the $n-$dimensional volume element. The Fourier components of the linear displacement field can be easily written in terms of the Fourier modes of the divergence field,

$$\Psi_L(\mathbf{k}) = \mathrm{i}\frac{\mathbf{k}}{k^2}\kappa_L(\mathbf{k}). \tag{23}$$

Note that because of the assumed statistical homogeneity and isotropy of space, ensemble average of products of two Fourier modes vanish for modes that do not sum to zero. This property holds for equal as well as unequal time correlators. In the following, we furthermore consider Gaussian initial conditions. As it will turn out, this is a crucial property. It indeed determines the diagrammatic structure and the contributions to the quantities of interest. Within this assumption the entire statistical properties of the initial density field are defined by its power spectrum, $P_0(\mathrm{k})$, such that:

$$\langle\kappa_0(\mathbf{k}_1)\kappa_0(\mathbf{k}_2)\rangle = \delta_\mathrm{D}(\mathbf{k}_1+\mathbf{k}_2)P_0(k_1), \tag{24}$$

where $\langle\,.\,\rangle$ represents ensemble averages over the statistical process at the origin of the large-scale structure.

If the notion of power spectrum has been widely used in theoretical and observational cosmology since the early eighties, the notion of propagator is relatively new. It has been introduced in [8] (see also [20] for the more general notion of response functions). By definition it represents the ensemble average of the functional derivative of a given cosmic field component with respect to the initial field value. What we will be interested in here is the propagator between an initial convergence mode $\kappa_0(\mathbf{k})$ and the final convergence mode $\kappa(\mathbf{k}',\eta)$ (the one defined with respect to the rotational parts vanishes for parity reasons in case of rotational-free initial conditions). As $\kappa(\mathbf{k}',\eta)$ is the result of a complex nonlinear process, it is formally a functional of the whole set of the initial density modes (only in the linear regime does it only depend on the same $\mathbf{k}$ mode). We can then introduce the functional derivative of $\kappa(\mathbf{k}',\eta)$ with respect to $\kappa_0(\mathbf{k})$: $\partial\kappa(\mathbf{k}',\eta)/\partial\kappa_0(\mathbf{k})$. This is a stochastic quantity whose ensemble average does not vanish for $\mathbf{k}=\mathbf{k}'$. It defines the *propagator* [22],

$$\langle\frac{\partial\kappa(\mathbf{k}',\eta)}{\partial\kappa_0(\mathbf{k})}\rangle = \delta_\mathrm{D}(\mathbf{k}-\mathbf{k}')G(k,\eta). \tag{25}$$

The goal of this paper is precisely to investigate the behavior of the propagator $G(k,\eta)$. In the linear regime the functional $\kappa[\kappa_0]$ is trivial and given by Eq.(21) which implies that,

$$G_L(k,\eta) = e^\eta. \tag{26}$$

From a perturbation theory point of view, the functional $\kappa[\kappa_0]$ can be expanded in terms of the initial convergence field,

$$\kappa(\mathbf{k},\eta) = \sum_{p=1}^{\infty}\int \mathrm{d}^n\mathbf{w}_1\ldots\mathrm{d}^n\mathbf{w}_p\,\delta_\mathrm{D}\left(\mathbf{k}-\sum_{i=1}^{p}\mathbf{w}_i\right) \times\mathcal{F}^{(p)}(\mathbf{w}_1,\ldots,\mathbf{w}_n;\eta)\,\kappa_0(\mathbf{w}_1)\ldots\kappa_0(\mathbf{w}_p) \tag{27}$$

where the kernels $\mathcal{F}^{(p)}$ are *symmetric* functions of wave modes. They are determined by the motion equations for κ and ω. Then we have

$$G(k,\eta) = \sum_p\int \mathrm{d}^n\mathbf{w}_1\ldots\mathrm{d}^n\mathbf{w}_{p-1} \times p\mathcal{F}^{(p)}(\mathbf{w}_1,\ldots,\mathbf{w}_{p-1},\mathbf{k};\eta)\,\langle\kappa_0(\mathbf{w}_1)\ldots\kappa_0(\mathbf{w}_{p-1})\rangle \tag{28}$$

(the ensemble average of the r.h.s. of this equation ensures that $\sum_{i=1}^{p-1}\mathbf{w}_i=0$ so that $\delta_\mathrm{D}(\mathbf{k}-\sum_{i=1}^{p}\mathbf{w}_i)$ is transformed into $\delta_\mathrm{D}(\mathbf{k}-\mathbf{k}')$). Such an expansion can be represented in a diagrammatic way by taking advantage of the Gaussian initial conditions. This can serve as a basis for resummation schemes. We shall illustrate this construction for the 2D Lagrangian dynamics first.

III. 2D DYNAMICS

The aim of this section is to derive explicitly the motion equations for the Lagrangian 2D dynamics and to explore the resulting propagator properties. Since its mathematical structure is simpler than for the 3D case, it serves to illustrate the method we develop here to compute the propagators.

A. Decomposition over curl-free and divergence-less parts

We investigate in this section the simpler case of a two-dimensional dynamics. This corresponds to perturbations with $\Psi_3=0$ that do not depend on the third coordinate, q_3 or x_3. Therefore, the nonlinear dynamics is restricted to the plane $(\mathbf{e}_1,\mathbf{e}_2)$ and particles exactly follow the Hubble expansion along the third axis $\mathbf{e}_3$. Then, it is convenient to decompose the Lagrangian displacement field over a curl-free part χ and a divergence-less part λ as

$$\Psi = \begin{pmatrix}\Psi_1\\ \Psi_2\\ 0\end{pmatrix} = \begin{pmatrix}\frac{\partial\chi}{\partial q_1}+\frac{\partial\lambda}{\partial q_2}\\ \frac{\partial\chi}{\partial q_2}-\frac{\partial\lambda}{\partial q_1}\\ 0\end{pmatrix} = \nabla_\mathbf{q}.\chi+\nabla_\mathbf{q}\times(\lambda\,\mathbf{e}_3). \tag{29}$$

Here and in the following we note × the 3-dimensional vector product. Then, the divergence $-\kappa$ reads

$$\kappa = -\nabla^2_\mathbf{q}\chi, \quad \kappa(\mathbf{k}) = k^2\chi(\mathbf{k}). \tag{30}$$

In a similar fashion, we define the vorticity as

$$\omega = -\nabla^2_\mathbf{q}\lambda, \quad \omega(\mathbf{k}) = k^2\lambda(\mathbf{k}). \tag{31}$$

Then, the equation of motion (9) reads in Fourier space as

$$\begin{aligned}\kappa'' + \frac{1}{2}\kappa' - \frac{3}{2}\kappa = & \int \mathrm{d}\mathbf{k}_1 \mathrm{d}\mathbf{k}_2 \, \delta_{\mathrm{D}}(\mathbf{k}_1+\mathbf{k}_2-\mathbf{k}) \\ & \times \left\{ \alpha(\mathbf{k}_1,\mathbf{k}_2) \left[\kappa_1(\kappa_2''+\frac{1}{2}\kappa_2'-\frac{3}{4}\kappa_2) + \omega_1(\omega_2''+\frac{1}{2}\omega_2'-\frac{3}{4}\omega_2) \right] \right. \\ & \left. + \beta(\mathbf{k}_1,\mathbf{k}_2) \left[\omega_1(\kappa_2''+\frac{1}{2}\kappa_2') - \kappa_1(\omega_2''+\frac{1}{2}\omega_2') + \frac{3}{2}\kappa_1\omega_2 \right] \right\} \end{aligned} \tag{32}$$

where we noted $\kappa_i = \kappa(\mathbf{k}_i), \omega_i = \omega(\mathbf{k}_i)$, and we introduced the symmetric kernels

$$\alpha(\mathbf{k}_1,\mathbf{k}_2) = \frac{\det(\mathbf{k}_1,\mathbf{k}_2)^2}{k_1^2 k_2^2}, \tag{33}$$

$$\beta(\mathbf{k}_1,\mathbf{k}_2) = \frac{(\mathbf{k}_1.\mathbf{k}_2)\det(\mathbf{k}_1,\mathbf{k}_2)}{k_1^2 k_2^2}, \tag{34}$$

with

$$\det(\mathbf{k}_1,\mathbf{k}_2) = k_{1,1}k_{2,2} - k_{1,2}k_{2,1} = \mathbf{e}_3.(\mathbf{k}_1 \times \mathbf{k}_2). \tag{35}$$

It is to be noted that, unlike their Eulerian counterparts, these kernels only depend on the relative angle between the wave modes.

Equation (32) can be written in integral form by using the Green's function $\mathcal{G}(\eta,\eta')$ that is solution of

$$\left(\frac{\mathrm{d}^2}{\mathrm{d}\eta^2} + \frac{1}{2}\frac{\mathrm{d}}{\mathrm{d}\eta} - \frac{3}{2} \right) \mathcal{G}(\eta,\eta') = \delta_{\mathrm{D}}(\eta-\eta'). \tag{36}$$

It reads as

$$\mathcal{G}(\eta,\eta') = \theta(\eta-\eta')\frac{2}{5}\left[e^{(\eta-\eta')} - e^{-3(\eta-\eta')/2} \right], \tag{37}$$

where $\theta(\eta-\eta')$ is the Heaviside factor which enforces causality. This constraint fully determines $\mathcal{G}(\eta,\eta')$ (whereas Eq.(36) alone does not select between advanced and retarded propagators or combinations of both). Of course, in Eq.(37) we recognize the two linear modes of Eq.(20). Thus, we can write the solution of Eq.(32) as:

$$\begin{aligned}\kappa = \kappa_L + & \int_{-\infty}^{\eta} \mathrm{d}\eta' \mathcal{G}(\eta,\eta') \int \mathrm{d}\mathbf{k}_1 \mathrm{d}\mathbf{k}_2 \, \delta_{\mathrm{D}}(\mathbf{k}_1+\mathbf{k}_2-\mathbf{k}) \\ & \times \left\{ \alpha(\mathbf{k}_1,\mathbf{k}_2) \left[\kappa_1(\kappa_2''+\frac{1}{2}\kappa_2'-\frac{3}{4}\kappa_2) + \omega_1(\omega_2''+\frac{1}{2}\omega_2'-\frac{3}{4}\omega_2) \right] \right. \\ & \left. + \beta(\mathbf{k}_1,\mathbf{k}_2) \left[\omega_1(\kappa_2''+\frac{1}{2}\kappa_2') - \kappa_1(\omega_2''+\frac{1}{2}\omega_2') + \frac{3}{2}\kappa_1\omega_2 \right] \right\} \end{aligned} \tag{38}$$

where all terms in the brackets are taken at time η' in the past.

On the other hand, the curl-free Eulerian velocity constraint (13) reads as

$$\begin{aligned}\omega' = & \int \mathrm{d}\mathbf{k}_1 \mathrm{d}\mathbf{k}_2 \delta_{\mathrm{D}}(\mathbf{k}_1+\mathbf{k}_2-\mathbf{k}) \left\{ \alpha(\mathbf{k}_1,\mathbf{k}_2)[\kappa_1\omega_2' - \omega_1\kappa_2'] \right. \\ & \left. + \beta(\mathbf{k}_1,\mathbf{k}_2)\left[\kappa_1\kappa_2' + \omega_1\omega_2'\right] \right\}. \end{aligned} \tag{39}$$

From Sect. II B we can see that the linear vorticity vanishes, $\omega_L = 0$, and Eq.(39) can be integrated as

$$\begin{aligned}\omega = & \int_{-\infty}^{\eta} \mathrm{d}\eta' \int \mathrm{d}\mathbf{k}_1 \mathrm{d}\mathbf{k}_2 \delta_{\mathrm{D}}(\mathbf{k}_1+\mathbf{k}_2-\mathbf{k}) \left\{ \alpha(\mathbf{k}_1,\mathbf{k}_2) \right. \\ & \left. \times [\kappa_1\omega_2' - \omega_1\kappa_2'] + \beta(\mathbf{k}_1,\mathbf{k}_2)\left[\kappa_1\kappa_2' + \omega_1\omega_2'\right] \right\}. \end{aligned} \tag{40}$$

In Eqs.(38) and (40) we have set up the initial conditions at time $\eta_I \to -\infty$. It would be possible to keep η_I finite, but this introduces extra terms in the perturbative series for κ and ω that involve the decaying mode κ_- of Eq.(20). By contrast, from Eqs.(38), (40), the nonlinear quantities κ and ω can be written as a perturbative series over powers of the linear growing mode $e^{\eta}\,\kappa_0$, such that the term of order p factorizes as $e^{p\eta}\,\kappa^{(p)}(\mathbf{k})$, as in the standard perturbation theory.

The kernels $\alpha(\mathbf{k}_1,\mathbf{k}_2)$ and $\beta(\mathbf{k}_1,\mathbf{k}_2)$ obey the symmetries

$$\alpha(\mathbf{k}_1,\mathbf{k}_2) = \alpha(\mathbf{k}_2,\mathbf{k}_1), \;\; \beta(\mathbf{k}_1,\mathbf{k}_2) = -\beta(\mathbf{k}_2,\mathbf{k}_1), \tag{41}$$

as seen from Eqs.(33)-(35). This is consistent with the fact that κ and χ are scalars whereas ω and λ are pseudoscalars, as seen from Eq.(29) (so that $\nabla_{\mathbf{q}} \times (\lambda\,\mathbf{e}_3)$ is a vector like Ψ). Then, under parity $\mathcal{P}$ we have:

$$\mathcal{P} : \kappa \to \kappa, \;\omega \to -\omega, \;\alpha \to \alpha, \;\beta \to -\beta. \tag{42}$$

Equation (42) actually implies that the kernels α, β, satisfy Eq.(41), since the exchange of basis vectors $\mathbf{e}_1 \leftrightarrow \mathbf{e}_2$ can be written as a rotation followed by a reflection. Then, the symmetry (42) directly determines which kernel α or β is associated with a factor such as $\kappa\kappa$ or $\kappa\omega$ in Eqs.(32) and (39).

B. Diagrammatic representation

The equations (38, 40) have a simple diagrammatic representation which illustrates the fact that the functions $\mathcal{F}^{(p)}$ are obtained from successive quadratic interactions. A diagrammatic expansion of equations (38, 40) is presented in Fig. 1. Each open circle stands for a linear growing mode doublet $\{\kappa_L, \omega_L\} = \{e^{\eta_j}\kappa_0(\mathbf{k}_j), 0\}$, whereas the vertex points represent the interaction operators that can be read out from Eqs.(38, 40). For instance, its first component (the one that represents $\{\kappa(\mathbf{k}_1,\eta_1), \;\kappa(\mathbf{k}_2,\eta_2)\} \to \kappa(\mathbf{k},\eta)$) is

$$\begin{aligned}\gamma_{111}(\mathbf{k},\eta;\mathbf{k}_1,\eta_1,\mathbf{k}_2,\eta_2) = & \int \mathrm{d}\eta' \mathcal{G}(\eta,\eta')\delta_{\mathrm{D}}(\mathbf{k}-\mathbf{k}_1-\mathbf{k}_2) \\ & \times \delta_{\mathrm{D}}(\eta_1-\eta')\delta_{\mathrm{D}}(\eta_2-\eta') \left(\frac{\partial^2}{\partial\eta_2^2} + \frac{1}{2}\frac{\partial}{\partial\eta_2} - \frac{3}{4} \right). \end{aligned} \tag{43}$$

Then, one must integrate over the coordinates $(\mathbf{k}_j, \eta_j)$ of the incoming modes at each vertex.

As noted in [13], each of these diagrams exhibits one and only one "principal line": a line that runs from the initial time to the final time without crossing a circle. It

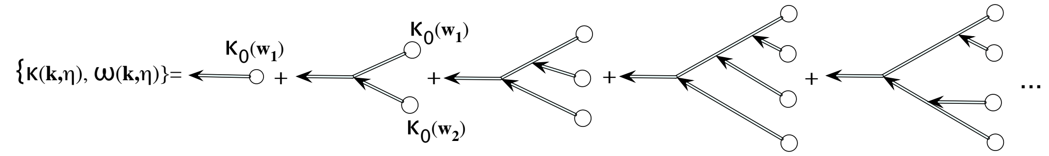

FIG. 1: Diagrammatic expression of the expansion of the convergence-vorticity doublet, $\{\kappa(\mathbf{k},\eta),\omega(\mathbf{k},\eta)\}$, in 2D dynamics. See text for details.

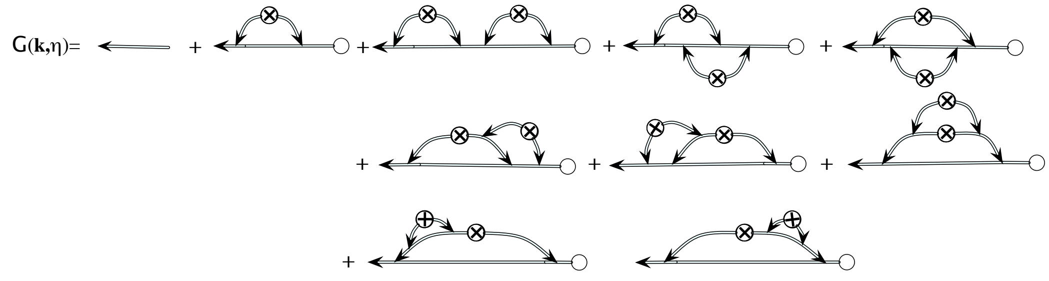

FIG. 2: Diagrammatic expression of the expansion of the propagator $G(k,\eta)$ in 2D dynamics. All the contribution up to 2 loops are included. Note that the last two rows correspond to loop configurations that do not all connect to the "principal line" (shown here as a straight horizontal line). These are the contribution we assume to be subdominant. See text for details.

is then possible to sort the loop terms with respect to the number of vertices that are attached to this line. It is then expected that in the high-k limit the dominant contribution comes from the diagrams whose number of such vertices are larger (see [13] for details). As seen in [16] and recalled below, this can be justified in a certain regime if it is possible to have a large separation of scales. In the following, we will restrict our calculations to this subset of contributions. For instance, for the terms up to two-loop order, they correspond to the first row of Fig. 2. It is important to note that these diagrams are such that the incoming waves are always in the linear regime. In [13], the authors were able to resum these loop contributions (basically by properly counting them). In a Lagrangian description things are made more difficult because of the complex nature of the vertices and it is not always possible to obtain an explicit analytical formula for this resummed propagator.

However, as shown in [16], the propagator defined by this partial series of diagrams can be seen as the exact propagator of a simpler dynamics (that only gives rise to these diagrams). The latter can be derived by linearizing the equations of motion in a certain fashion. Then, we can compute the propagator $G(k,\eta)$ by solving exactly this second dynamics and next performing the average over the initial conditions. This can be made numerically without performing diagrammatic resummations. We first illustrate this alternative method for the 2D-Lagrangian dynamics.

C. High-k approximation

1. *Resummation of dominant diagrams*

As stated above, the dominant diagrams are expected to be those where all incoming lines to the principal path are in the linear regime. Following [16], such a system is described by motion equations similar to (38) and (40), where in the terms in the right hand sides we replace all terms except one by their linear values κ_L and ω_L (the latter vanishes here) and sum over all possible choices. These equations correspond to a physical system where it is legitimate to separate scales, for instance if there exists an upper wavenumber Λ so that most of the power is associated with small wavenumbers $w<\Lambda$. Then, in the limit $k\gg\Lambda$, the evolution of a given mode $\mathbf{k}$ is governed by the contributions of small wavenumbers, $k_1<\Lambda$ (whence $k_2\simeq k$) or $k_2<\Lambda$ (whence $k_1\simeq k$), in the right hand side of Eqs.(32) and (39), that are further assumed to be in the linear regime.

The motion equations for the high-$\mathbf{k}$ modes then form a set of *linear* equations in presence of a random background described by the collection of the low-$\mathbf{w}_j$ modes. This leaves us with still a complicated system of equations to solve. A dramatic simplification can further be made because of the high-k limit. Indeed, since $k\gg w_j$, $\mathbf{w}_j$ denoting the incoming linear wave modes, the wave mode $\mathbf{k}$ is almost left unchanged along the principal line (in other words one is entitled to replace $\delta_{\rm D}(\mathbf{k}'+\mathbf{w}_j-\mathbf{k})$ in each vertex point by $\delta_{\rm D}(\mathbf{k}'-\mathbf{k})$). In this context, the motion equations that describe the mode evolution, Eqs.(32) and (39), can by approximated by,

$$\kappa''(\mathbf{k},\eta)+\frac{1}{2}\kappa'(\mathbf{k},\eta)-\frac{3}{2}\kappa(\mathbf{k},\eta) = \int \mathrm{d}\mathbf{w}\ \kappa_L(\mathbf{w},\eta)\left\{\alpha(\mathbf{k},\mathbf{w})\left[\kappa''(\mathbf{k},\eta)+\frac{1}{2}\kappa'(\mathbf{k},\eta)\right] +\beta(\mathbf{k},\mathbf{w})\left[\omega''(\mathbf{k},\eta)+\frac{1}{2}\omega'(\mathbf{k},\eta)\right]\right\}, \tag{44}$$

$$\omega'(\mathbf{k},\eta) = \int \mathrm{d}\mathbf{w}\ \kappa_L(\mathbf{w},\eta)\{\alpha(\mathbf{k},\mathbf{w})[\omega'(\mathbf{k},\eta)-\omega(\mathbf{k},\eta)]+\beta(\mathbf{k},\mathbf{w})[\kappa(\mathbf{k},\eta)-\kappa'(\mathbf{k},\eta)]\}, \tag{45}$$

so that high-k modes now evolve *independently* on one another. One can easily check that the solution of Eqs.(44)-(45), written as a perturbative series over κ_0, gives back the principal-path diagrams described above (here with the approximation $\mathbf{k}'=\mathbf{k}$).

Of course, we could apply the same procedure to the equations of motion (38),(40), written in the integral form [12, 16]. This is equivalent to the differential form used above, but it is less convenient for practical purposes. For instance, it is easier to solve numerically the differential equations (44)-(45) than their integral equivalents which require the computation of an integral over all past values to advance to the next time-step.

Then, we note from Eqs.(44)-(45) that all contributions from the incoming waves $\kappa_L(\mathbf{w}_j)$ can be factorized out and resummed in two distinct bundles of waves, $\hat{\alpha}$ and $\hat{\beta}$, defined as,

$$\hat{\alpha}(\mathbf{k})=\int \mathrm{d}\mathbf{w}\ \kappa_0(\mathbf{w})\alpha(\mathbf{k},\mathbf{w}),\qquad \hat{\beta}(\mathbf{k})=\int \mathrm{d}\mathbf{w}\ \kappa_0(\mathbf{w})\beta(\mathbf{k},\mathbf{w}), \tag{46}$$

such that Eqs.(44)-(45) now read,

$$\kappa''(\mathbf{k},\eta)+\frac{1}{2}\kappa'(\mathbf{k},\eta)-\frac{3}{2}\kappa(\mathbf{k},\eta) = e^{\eta}\hat{\alpha}(\mathbf{k})\left(\kappa''(\mathbf{k},\eta)+\frac{1}{2}\kappa'(\mathbf{k},\eta)\right)+e^{\eta}\hat{\beta}(\mathbf{k})\left(\omega''(\mathbf{k},\eta)+\frac{1}{2}\omega'(\mathbf{k},\eta)\right) \tag{47}$$

$$\omega'(\mathbf{k},\eta) = -e^{\eta}\hat{\beta}(\mathbf{k})(\kappa'(\mathbf{k},\eta)-\kappa(\mathbf{k},\eta))+e^{\eta}\hat{\alpha}(\mathbf{k})(\omega'(\mathbf{k},\eta)-\omega(\mathbf{k},\eta)). \tag{48}$$

In other words, the fields $\kappa(\mathbf{k})$ and $\omega(\mathbf{k})$ depend on the linear modes only through the combinations $\hat{\alpha}$ and $\hat{\beta}$. This introduces a dramatic simplification because then the ensemble average of Eq.(25) can be performed through a simple average over the two variables $\hat{\alpha}$ and $\hat{\beta}$. Since Eqs.(47)-(48) are linear the solution is proportional to $\kappa_0(\mathbf{k})$. It is convenient to write it as,

$$\kappa(\mathbf{k},\eta)=e^{\eta}\kappa_0(\mathbf{k})\ \hat{\kappa}(\eta), \tag{49}$$

$$\omega(\mathbf{k},\eta)=e^{\eta}\kappa_0(\mathbf{k})\ \hat{\omega}(\eta). \tag{50}$$

As a consequence, we have

$$G(k,\eta)=e^{\eta}\hat{G}(\eta)\quad\text{with}\quad \hat{G}(\eta)=\langle\hat{\kappa}(\eta)\rangle. \tag{51}$$

We can already note that because $\hat{\alpha}$ and $\hat{\beta}$ depend on the direction of $\mathbf{k}$ only, $\hat{G}(\eta)$ will be completely independent of $\mathbf{k}$ (since a priori it could only depend on its norm).

In the last equation (51) the ensemble average now reduces to the computation of the expectation value of $\hat{\kappa}(\eta)$ with respect to the distribution of $\hat{\alpha}$ and $\hat{\beta}$. We then need to explore a bit more the statistical properties of $\hat{\alpha}$ and $\hat{\beta}$. Using the fact that the linear density field $\delta_L(\mathbf{q})=\kappa_L(\mathbf{q})$ is real, hence $\kappa_0(\mathbf{w})^*=\kappa_0(-\mathbf{w})$, it can be easily checked that $\hat{\alpha}$ and $\hat{\beta}$ are real numbers. Moreover, we can see from Eqs.(46) that they are independent Gaussian random variables with:

$$\langle\hat{\alpha}^2\rangle=3\sigma_2^2,\ \ \langle\hat{\beta}^2\rangle=\sigma_2^2,\ \ \langle\hat{\alpha}\hat{\beta}\rangle=0, \tag{52}$$

with,

$$\sigma_2^2=\frac{\pi}{4}\int_0^{\infty}\mathrm{d}w\, wP_0(w). \tag{53}$$

Note that $8\sigma_2^2$ is also the variance of the density contrast $\langle\delta(\mathbf{x})^2\rangle$. The joint distribution function of $\hat{\alpha}$ and $\hat{\beta}$ is then

$$\mathcal{P}(\hat{\alpha},\hat{\beta})\,\mathrm{d}\hat{\alpha}\,\mathrm{d}\hat{\beta}=\frac{\mathrm{d}\hat{\alpha}\,\mathrm{d}\hat{\beta}}{\sqrt{3}2\pi\sigma_2^2}\exp\left[-\frac{\hat{\alpha}^2}{6\sigma_2^2}-\frac{\hat{\beta}^2}{2\sigma_2^2}\right]. \tag{54}$$

As a result we simply have,

$$\hat{G}(\eta)=\int_{-\infty}^{\infty}\hat{\kappa}(\eta;\hat{\alpha},\hat{\beta})\mathcal{P}(\hat{\alpha},\hat{\beta})\,\mathrm{d}\hat{\alpha}\,\mathrm{d}\hat{\beta}, \tag{55}$$

where $\hat{\kappa}(\eta;\hat{\alpha},\hat{\beta})$ is the solution of the system (47)-(48), written in terms of $\hat{\kappa}$ and $\hat{\omega}$, parameterized by the coefficients $\hat{\alpha},\hat{\beta}$. The calculation of the propagator can take advantage of the symmetries (42). In particular, we have:

$$\hat{\kappa}(\eta;\hat{\alpha},\hat{\beta})=\hat{\kappa}(\eta;\hat{\alpha},-\hat{\beta}),\ \ \hat{\omega}(\eta;\hat{\alpha},\hat{\beta})=-\hat{\omega}(\eta;\hat{\alpha},-\hat{\beta}). \tag{56}$$

We can also note that for $\mu>0$,

$$\hat{\kappa}(\eta;\mu\hat{\alpha},\mu\hat{\beta}) = \hat{\kappa}(\eta+\ln\mu;\hat{\alpha},\hat{\beta}) \tag{57}$$

$$\hat{\omega}(\eta;\mu\hat{\alpha},\mu\hat{\beta}) = \hat{\omega}(\eta+\ln\mu;\hat{\alpha},\hat{\beta}). \tag{58}$$

2. Behavior of the propagator $G(k,\eta)$

The asymptotic behavior of $G(k,\eta)$ is intimately related to the behavior of the solutions of (47)-(48) for finite values of the parameters $\hat\alpha$ and $\hat\beta$. This can be inferred by inspection of these differential equations. Thus, looking for an asymptotic power-law solution, $\hat\kappa \sim \hat\kappa_\infty e^{\nu\eta}$ and $\hat\omega \sim \hat\omega_\infty e^{\nu\eta}$, in the limit of large η where the right hand side dominates in Eqs. (47)-(48), we obtain the condition

$$\begin{vmatrix} \hat\alpha(\nu+1)(\nu+\frac{3}{2}) & \hat\beta(\nu+1)(\nu+\frac{3}{2}) \\ -\hat\beta\nu & \hat\alpha\nu \end{vmatrix} = (\hat\alpha^2+\hat\beta^2)\nu(\nu+1)(\nu+\frac{3}{2}) = 0, \tag{59}$$

which gives the asymptotic modes:

$$\nu_1 = 0, \quad \nu_2 = -1, \quad \nu_3 = -\frac{3}{2}. \tag{60}$$

In fact, the mode ν_2 can be removed since Eq.(47) can be integrated once, as shown in Eq.(A4) in the appendix. Therefore, when $\eta \gg 1$, $\hat\kappa$ and $\hat\omega$ are expected to be constant (their value depending on the parameters $\hat\alpha$ and $\hat\beta$ in a complicated way) because of the mode ν_1. This implies that the propagator $\hat G$ obtained from the Gaussian integration (55) must also be constant at late time. This expected behavior assumes that the differential equations (47)-(48) do not encounter a singularity at a finite time η. We can check that Eqs. (47)-(48) do not show explicit singularities associated with zeros of the coefficient of the higher-order terms. Indeed, the determinant of the coefficients of highest-order derivatives reads as

$$\begin{vmatrix} 1-\hat\alpha e^\eta & -\hat\beta e^\eta \\ \hat\beta e^\eta & 1-\hat\alpha e^\eta \end{vmatrix} = (1-\hat\alpha e^\eta)^2 + (\hat\beta e^\eta)^2 \tag{61}$$

which never vanishes if $\hat\beta \neq 0$. We have checked numerically that the system of differential equations (47)-(48) obeys the behavior described above, with no singularity and a constant asymptote a late time. This is depicted in Fig. 5 with a 2D plot of $\hat\kappa(\eta;\hat\alpha,\hat\beta)$ over the plane $(\hat\alpha,\hat\beta)$ at time $\eta = 0$ (this 2D plot is sufficient to fully determine the behavior of $\hat\kappa(\eta;\hat\alpha,\hat\beta)$ thanks to the scaling law (57)).

We show in Fig. 3 our results for the propagator $\hat G(\eta)$ obtained from the numerical integration of Eq.(55). We can see that it first grows until it reaches a maximum at $\eta \sim 0$ and next decreases to converge to a constant $\hat G(\eta = \infty) \sim 0.8$, a behavior qualitatively in agreement with the discussion above. Note that at early times the rise of $\hat G$ means that the propagator $G(k,\eta)$ grows faster than the linear prediction (26), until $\eta \sim 1$.

The 2D case described above illustrates the power of the method based on associating the series of principal-path diagrams with a linear dynamics as in Eqs.(47)-(48). Indeed, in the high-k limit the dependence on initial conditions is reduced to a few random parameters (here $\hat\alpha$ and $\hat\beta$), as can also be read from the diagrams of Figs. 1. Then, the ensemble average is reduced to ordinary integrals (55) (instead of path integrals over the field $\kappa_0(\mathbf{k})$) and the resummation associated with the infinite series of diagrams is obtained by computing the exact solution of the differential equations Eqs.(47)-(48). Both steps can be performed numerically, as above, since they only involve ordinary integrals and differential equations (instead of functionals of fields). This allows us to compute the propagator $G(k,\eta)$ even when the diagrammatic series cannot be exactly resummed by analytical formulae (which corresponds to the case when the differential equations (47)-(48) have no known explicit solutions). Moreover, even in this case, we can obtain exact analytical results for the late-time non-perturbative behavior of the propagator, as in Eqs.(60), by direct inspection of the effective linear equations of motion (47)-(48).

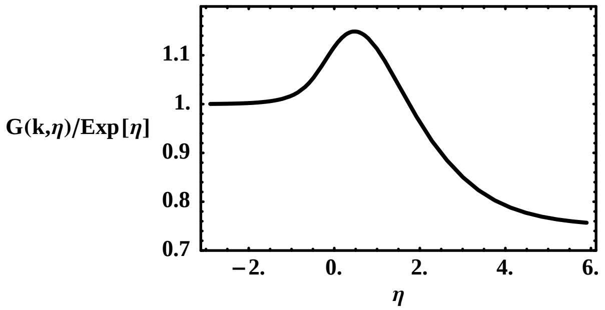

FIG. 3: The propagator $\hat G(\eta)$ as a function of η. It is obtained from Eq.(55) for a variance $\sigma_2 = 1$. Note that $\hat G(\eta)$ depends only on the reduced variable $\eta + \ln\sigma_2$ as a consequence of (57-58).

We further discuss the properties of the system (47)-(48) in appendix A. In particular, we show that taking into account the vorticity (i.e. $\hat\beta \neq 0$ and $\hat\omega \neq 0$) is necessary to obtain a well-behaved propagator at late times (otherwise a divergence appears), and that the perturbative series over powers of κ_0 is probably only asymptotic (i.e. with zero radius of convergence).

IV. 3D DYNAMICS

We now consider the case of the full 3D dynamics. This leads to slightly more intricate expressions as we have a few more degrees of freedom but we can still follow the analysis described in Sect. III for the simpler 2D dynamics. Moreover, we shall find that the results obtained in Sect. III remain valid.

First, as in Eq.(29), we can decompose the displacement field over a curl-free part χ and a divergence-less part $\vec{\lambda}$ as

$$\Psi = \begin{pmatrix} \frac{\partial\chi}{\partial q_1} + \frac{\partial\lambda_3}{\partial q_2} - \frac{\partial\lambda_2}{\partial q_3} \\ \frac{\partial\chi}{\partial q_2} + \frac{\partial\lambda_1}{\partial q_3} - \frac{\partial\lambda_3}{\partial q_1} \\ \frac{\partial\chi}{\partial q_3} + \frac{\partial\lambda_2}{\partial q_1} - \frac{\partial\lambda_1}{\partial q_2} \end{pmatrix} = \nabla_{\mathbf{q}}.\chi + \nabla_{\mathbf{q}} \times \vec{\lambda}. \quad (62)$$

Thus, the rotational part $\vec{\lambda}$ has now two degrees of freedom: there are three components $\lambda_1, \lambda_2, \lambda_3$, but the divergence of $\vec{\lambda}$ does not contribute and can be set to zero. As in Eqs.(30)-(31) we define the divergence $-\kappa$ and the vorticity $\vec{\omega}$ by

$$\kappa = -\nabla^2_{\mathbf{q}}\chi, \quad \vec{\omega} = -\nabla^2_{\mathbf{q}}\vec{\lambda}. \quad (63)$$

Then, the spatial derivatives of the displacement field read in Fourier space as

$$\frac{\partial\Psi_i}{\partial q_j} = \Psi_{i,j}(\mathbf{k}) = -\frac{k_i k_j}{k^2}\kappa(\mathbf{k}) - \epsilon_{ilm}\frac{k_j k_l}{k^2}\omega_m(\mathbf{k}), \quad (64)$$

where ϵ_{ilm} is the Levi-Civita symbol. Then, the equation of motion (9) reads in Fourier space as

$$\kappa'' + \frac{1}{2}\kappa' - \frac{3}{2}\kappa = \int \mathrm{d}\mathbf{k}_1\mathrm{d}\mathbf{k}_2\delta_{\mathrm{D}}(\mathbf{k}_1+\mathbf{k}_2-\mathbf{k}) \left\{ \frac{k_1^2k_2^2 - (\mathbf{k}_1.\mathbf{k}_2)^2}{k_1^2k_2^2}\kappa_1(\kappa_2'' + \frac{1}{2}\kappa_2' - \frac{3}{4}\kappa_2) - \frac{(\mathbf{k}_1.\mathbf{k}_2)}{k_1^2k_2^2}[\mathbf{k}_2.(\mathbf{k}_1 \times \vec{\omega}_1)](\kappa_2'' + \frac{1}{2}\kappa_2' - \frac{3}{2}\kappa_2) \right.$$
$$\left. - \frac{(\mathbf{k}_1.\mathbf{k}_2)}{k_1^2k_2^2}\kappa_1[\mathbf{k}_1.(\mathbf{k}_2 \times (\vec{\omega}_2'' + \frac{1}{2}\vec{\omega}_2'))] \right\} - \int \mathrm{d}\mathbf{k}_1\mathrm{d}\mathbf{k}_2\mathrm{d}\mathbf{k}_3\delta_{\mathrm{D}}(\mathbf{k}_1+\mathbf{k}_2+\mathbf{k}_3-\mathbf{k}) \left\{ \frac{\det(\mathbf{k}_1,\mathbf{k}_2,\mathbf{k}_3)^2}{2k_1^2k_2^2k_3^2}\kappa_1\kappa_2(\kappa_3'' + \frac{1}{2}\kappa_3' - \frac{1}{2}\kappa_3) \right.$$
$$\left. + \frac{\det(\mathbf{k}_1,\mathbf{k}_2,\mathbf{k}_3)}{k_1^2k_2^2k_3^2}[(\mathbf{k}_2 \times \mathbf{k}_3).(\mathbf{k}_1 \times \vec{\omega}_1)]\kappa_2(\kappa_3'' + \frac{1}{2}\kappa_3' - \frac{3}{4}\kappa_3) + \frac{\det(\mathbf{k}_1,\mathbf{k}_2,\mathbf{k}_3)}{2k_1^2k_2^2k_3^2}\kappa_1\kappa_2[(\mathbf{k}_1 \times \mathbf{k}_2).(\mathbf{k}_3 \times (\vec{\omega}_3'' + \frac{1}{2}\vec{\omega}_3'))] \right\} + .. (65)$$

where the dots stand for terms of order ω^2 and ω^3. We do not write these terms here since they will not contribute to the high-k approximation. The determinant $\det(\mathbf{k}_1,\mathbf{k}_2,\mathbf{k}_3)$ introduced in Eq.(65) is the determinant of the 3×3 matrix obtained by putting the coordinates of the vectors $\mathbf{k}_1, \mathbf{k}_2$ and $\mathbf{k}_3$, in the three columns. It is also given by:

$$\det(\mathbf{k}_1,\mathbf{k}_2,\mathbf{k}_3) = (\mathbf{k}_1 \times \mathbf{k}_2).\mathbf{k}_3 \quad (66)$$

Note that Eq.(65) is now cubic over Ψ, hence over κ, ω. For the constraints associated with the curl-free condition (12) we can use Eq.(15) which is still quadratic. This gives:

$$\frac{(\mathbf{k} \times \vec{\omega}') \times \mathbf{k}}{k^2} = \int \mathrm{d}\mathbf{k}_1\mathrm{d}\mathbf{k}_2\delta_{\mathrm{D}}(\mathbf{k}_1+\mathbf{k}_2-\mathbf{k})\frac{\mathbf{k}_1 \times \mathbf{k}_2}{k_1^2k_2^2}\{(\mathbf{k}_1.\mathbf{k}_2)\kappa_1\kappa_2' + \kappa_1[\mathbf{k}_1.(\mathbf{k}_2 \times \vec{\omega}_2')] + [\mathbf{k}_2.(\mathbf{k}_1 \times \vec{\omega}_1)]\kappa_2'\} + .. \quad (67)$$

where the dots stand for terms of order ω^2. We can check that only the combination $\mathbf{k}\times\vec{\omega}$ appears in Eqs.(65)-(67). Moreover, as in the 2D case where Eqs.(32)-(39) obeyed the parity symmetry (42), we can check that Eqs.(65)-(67) are consistent with the parity symmetry

$$\mathcal{P}: \quad \kappa \to \kappa, \quad \vec{\omega} \to \vec{\omega}. \quad (68)$$

In agreement with Eq.(62), $\vec{\lambda}$ and $\vec{\omega}$ are pseudovectors.

As in Sect. III C 1, the resummation associated with principal-path diagrams can be read from Eqs.(65)-(67) by linearizing over $\kappa, \vec{\omega}$. This yields

$$\kappa'' + \frac{1}{2}\kappa' - \frac{3}{2}\kappa = \int \mathrm{d}\mathbf{w}e^{\eta}\kappa_0(\mathbf{w}) \left\{ \frac{k^2w^2 - (\mathbf{k}.\mathbf{w})^2}{k^2w^2}(\kappa'' + \frac{1}{2}\kappa') - \frac{(\mathbf{k}.\mathbf{w})}{k^2w^2}[\mathbf{w}.(\mathbf{k} \times (\vec{\omega}'' + \frac{1}{2}\vec{\omega}'))] \right\}$$
$$- \int \mathrm{d}\mathbf{w}\mathrm{d}\mathbf{u}e^{2\eta}\kappa_0(\mathbf{w})\kappa_0(\mathbf{u}) \left\{ \frac{\det(\mathbf{k},\mathbf{w},\mathbf{u})^2}{2k^2w^2u^2}(\kappa'' + \frac{1}{2}\kappa' + \frac{3}{2}\kappa) + \frac{\det(\mathbf{k},\mathbf{w},\mathbf{u})}{2k^2w^2u^2}[(\mathbf{w} \times \mathbf{u}).(\mathbf{k} \times (\vec{\omega}'' + \frac{1}{2}\vec{\omega}' + \frac{3}{2}\vec{\omega}))] \right\} \quad (69)$$

and

$$\frac{(\mathbf{k}\times\vec{\omega}')\times\mathbf{k}}{k^2} = \int \mathrm{d}\mathbf{w} e^{\eta}\kappa_0(\mathbf{w})\frac{\mathbf{w}\times\mathbf{k}}{k^2 w^2} \times\{(\mathbf{k}.\mathbf{w})(\kappa'-\kappa)+[\mathbf{w}.(\mathbf{k}\times(\vec{\omega}'-\vec{\omega}))]\}\,. \quad (70)$$

As for the 2D case, each mode $\kappa(\mathbf{k}), \vec{\omega}(\mathbf{k})$ evolves independently of other high-k modes and the dependence on the initial field κ_0 is reduced to a few random parameters that can be written as integrals over κ_0. In order to make further progress, it is convenient to write Eqs.(69)-(70) in terms of coordinates. Without any loss of generality, we can choose $\mathbf{k}$ along the axis $\mathbf{e}_1$, and $\vec{\omega}$ in the plane $(\mathbf{e}_2, \mathbf{e}_3)$. Then, Eqs.(69)-(70) read as

$$\kappa''+\frac{1}{2}\kappa'-\frac{3}{2}\kappa = e^{\eta}(\tau_{22}+\tau_{33})(\kappa''+\frac{1}{2}\kappa') - e^{\eta}\tau_{13}(\omega_2''+\frac{1}{2}\omega_2') + e^{\eta}\tau_{12}(\omega_3''+\frac{1}{2}\omega_3') - e^{2\eta}(\tau_{22}\tau_{33}-\tau_{23}^2)(\kappa''+\frac{1}{2}\kappa'+\frac{3}{2}\kappa) - e^{2\eta}(\tau_{12}\tau_{23}-\tau_{22}\tau_{13})(\omega_2''+\frac{1}{2}\omega_2'+\frac{3}{2}\omega_2) + e^{2\eta}(\tau_{13}\tau_{23}-\tau_{33}\tau_{12})(\omega_3''+\frac{1}{2}\omega_3'+\frac{3}{2}\omega_3), \quad (71)$$

and:

$$\omega_2' = e^{\eta}\tau_{13}(\kappa'-\kappa)+e^{\eta}\tau_{33}(\omega_2'-\omega_2)-e^{\eta}\tau_{23}(\omega_3'-\omega_3), \quad (72)$$

$$\omega_3' = -e^{\eta}\tau_{12}(\kappa'-\kappa) - e^{\eta}\tau_{23}(\omega_2'-\omega_2) + e^{\eta}\tau_{22}(\omega_3'-\omega_3). \quad (73)$$

Here we introduced the symmetric parameters τ_{ij} defined by:

$$\tau_{ij} = \int \mathrm{d}\mathbf{w}\ \kappa_0(\mathbf{w})\frac{w_i\, w_j}{w^2}. \quad (74)$$

Using the property $\kappa_0(\mathbf{w})^* = \kappa_0(-\mathbf{w})$, we can see that the coefficients τ_{ij} are real random numbers. We recover the two-dimensional case (47)-(48) for

$$\tau_{i3}=0,\ \ \omega_2=0,\ \ \hat{\alpha}=\tau_{22},\ \ \hat{\beta}=\tau_{12}, \quad (75)$$

or

$$\tau_{i2}=0,\ \ \omega_3=0,\ \ \hat{\alpha}=\tau_{33},\ \ \hat{\beta}=-\tau_{13}. \quad (76)$$

Note that there are several symmetry properties. Two symmetries extend the property (56) obtained for the 2D case. They read as

$$\tau_{13}\to-\tau_{13},\ \tau_{23}\to-\tau_{23},\ \omega_2\to-\omega_2, \quad (77)$$

and

$$\tau_{12}\to-\tau_{12},\ \tau_{23}\to-\tau_{23},\ \omega_3\to-\omega_3, \quad (78)$$

where we only write the quantities that change under these two symmetries. A further symmetry comes from the invariance over a coordinate rotation in the $(\mathbf{e}_2, \mathbf{e}_3)$ plane. To express it, we can define the following quantities,

$$\tau = \frac{\tau_{22}+\tau_{33}}{2}, \quad (79)$$

$$\mathbf{v} = v\ e^{\mathrm{i}\theta_v} = \tau_{12}+\mathrm{i}\tau_{13}, \quad (80)$$

$$\vec{\gamma} = \gamma\ e^{2\mathrm{i}\theta_\gamma} = \frac{\tau_{22}-\tau_{33}}{2}+\mathrm{i}\tau_{23}, \quad (81)$$

which behave respectively like spin 0, 1 and 2 complex numbers with respect to coordinate rotations in the $(\mathbf{e}_2, \mathbf{e}_3)$ plane. The ensemble average of those quantities can be expressed in terms of σ_3^2 defined as,

$$\sigma_3^2 = \frac{8\pi}{15}\int \mathrm{d}w\, w^2 P_0(w), \quad (82)$$

with

$$\langle\tau^2\rangle = \langle|\mathbf{v}|^2\rangle = \langle|\vec{\gamma}|^2\rangle = \sigma_3^2, \quad (83)$$

while cross-correlations between these quantities vanish. We also define the complex vorticity ω as

$$\omega = -\omega_3 + \mathrm{i}\omega_2, \quad (84)$$

which is of spin 1 like $\mathbf{v}$. Here we use the fact that, as in the 2D case, Eqs.(71)-(73) are linear so that we can factorize a factor $\kappa_0(\mathbf{k})$, as in Eqs.(49)-(50). Then, the reduced quantities $\kappa/\kappa_0, \omega_i/\kappa_0$, are real (since the coefficients τ_{ij} of Eq.(74) are real) so that the complex vorticity (84) fully determines the doublet $\{\omega_2, \omega_3\}$. Then, the two equations (72)-(73) can be gathered into

$$\omega' = e^{\eta}\mathbf{v}(\kappa'-\kappa) + e^{\eta}\tau(\omega'-\omega) + e^{\eta}\vec{\gamma}(\omega'-\omega)^*, \quad (85)$$

whereas Eq.(71) reads as

$$\kappa''+\frac{1}{2}\kappa'-\frac{3}{2}\kappa \;=\; e^{\eta}2\tau(\kappa''+\frac{1}{2}\kappa')-e^{\eta}\frac{\mathbf{v}^*}{2}(\omega''+\frac{1}{2}\omega')-e^{\eta}\frac{\mathbf{v}}{2}(\omega''+\frac{1}{2}\omega')^*-e^{2\eta}(\tau^2-\vec{\gamma}\vec{\gamma}^*)(\kappa''+\frac{1}{2}\kappa'+\frac{3}{2}\kappa)$$
$$-e^{2\eta}\frac{\mathbf{v}\vec{\gamma}^*-\tau\mathbf{v}^*}{2}(\omega''+\frac{1}{2}\omega'+\frac{3}{2}\omega)-e^{2\eta}\frac{\mathbf{v}^*\vec{\gamma}-\tau\mathbf{v}}{2}(\omega''+\frac{1}{2}\omega'+\frac{3}{2}\omega)^*. \tag{86}$$

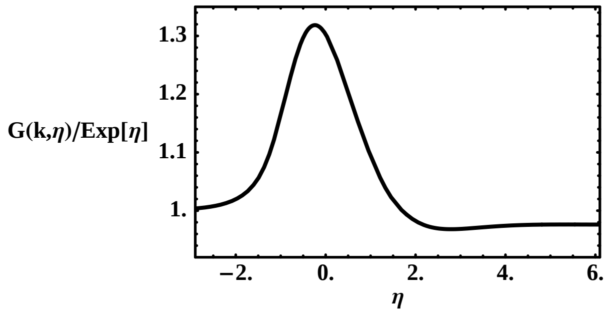

FIG. 4: The propagator $\hat{G}(\eta)$ as a function of η for the 3D dynamics. It is obtained for a variance $\sigma_3 = 1$.

We can see that all terms in Eq.(85) are of spin 1, whereas all terms in Eq.(86) are of spin 0. This clearly shows that these equations are invariant through rotations in the $(\mathbf{e}_2, \mathbf{e}_3)$ plane. Moreover, we can check that both sides in Eq.(86) are real. Obviously, the results depend only on the angle difference $\theta_v - \theta_\gamma$.

Finally, the scaling laws (57)-(58) also extend to the 3D case as

$$\mu > 0: \quad \tau_{ij} \to \mu\tau_{ij}, \;\; \eta \to \eta - \ln\mu. \tag{87}$$

As for the 2D case analized in Sect. III C 2, we can look for singularities associated with zeros of the determinant of the coefficients of higher-order derivatives. This gives from Eqs.(85)-(86):

$$\Delta = \left[(1-e^{\eta}\tau)^2 - e^{2\eta}|\vec{\gamma}|^2\right]^2 + \left|e^{\eta}\mathbf{v} + e^{2\eta}(\mathbf{v}^*\vec{\gamma} - \tau\mathbf{v})\right|^2 \tag{88}$$

The determinant Δ can only vanish if $|\vec{\gamma}| = 0$, or $|\mathbf{v}| = 0$, or $\theta_v - \theta_\gamma = n\pi/2$ with n integer, which is a region of zero measure in the space spanned by the coefficients $\tau, \mathbf{v}$, and $\vec{\gamma}$. We have checked numerically that the differential system is otherwise well-behaved and the ensemble averages lead to well-defined quantities. As in Eqs.(59)-(60), the asymptotic behavior of the solutions $\kappa, \omega_2, \omega_3$, can be read from the differential equations (71)-(73) by looking for asymptotic power-laws. This yields for the reduced variables $\hat{\kappa}, \hat{\omega}_2, \hat{\omega}_3$, defined as in Eqs.(49)-(50), the three asymptotic modes:

$$\nu_1 = 0, \;\; \nu_2 = \frac{-5 - \mathrm{i}\sqrt{23}}{4}, \;\; \nu_3 = \frac{-5 + \mathrm{i}\sqrt{23}}{4}. \tag{89}$$

Therefore, the reduced propagator $\hat{G}(\eta)$ must go to a constant at late times, as for the 2D case. Our numerical results are shown in Fig. 4 and we can see that they agree with this analysis. Thus, it appears that the 3D propagator exhibits the same features as the 2D case, with an early rise that is faster than the linear prediction and a late-time behavior that follows the linear power-law $G(\eta) \sim e^{\eta}$ (with a "renormalized" amplitude that is smaller than unity).

As for the 2D case (see Eq.(53)), the key quantity σ_3^2 that measures the amplitude of the fluctuations and the state of gravitational clustering, see Eqs.(82)-(83), is proportional to the variance of the density field $\langle\delta(\mathbf{x})^2\rangle$. We can note that for a CDM power spectrum it shows a logarithmic UV divergence (since $P_0(w) \sim w^{-3}$ at high w). Therefore, our results rigorously apply to linear power spectra with a high-k cutoff such that σ_3^2 is finite. However, since the fluid description does not hold beyond shell-crossing it could be argued that integrals such as (82) should be cut at the scale associated with the transition to nonlinearity in any case. On the other hand, within the high-k approximation studied in this article, the quantity σ_3 of Eq.(82) should be interpreted as the variance of the larger-scale density contrast, rather than the variance of the one-point density contrast. Indeed, we can see from Eq.(74) that the quantity which governs the coefficients τ_{ij} is the density contrast at the origin $\delta(\mathbf{x}=0)$ (discarding the angular dependence associated with w_iw_j/w^2). This in turn gives rise to Eq.(82). Mathematically, the specific role played by the origin is related to the breakdown of the invariance through translations entailed by the approximation $\delta_D(\mathbf{k}_1+\mathbf{k}_2-\mathbf{k}) \simeq \delta_D(\mathbf{k}_1-\mathbf{k})$ discussed in section III C 1. However, it is clear that within this approximation, based on a separation of scales between low wavenumbers $w < \Lambda$ and high wavenumbers $k \gg \Lambda$, any point located at a distance below $1/\Lambda$ from the origin could as well be chosen as a reference. In other words, within this high-k approximation, σ_3^2 should be understood as the variance of the larger-scale density contrast, associated with wavenumbers $w < \Lambda$ (and $\Lambda < k$). Then, in Eq.(82) we relaxed the cutoff Λ, which is valid for linear power spectra with small high-k power so that the integral converges (and the high-k approximation discussed in section III C 1 can make sense). We can see that CDM power spectra are at the limit of applicability of this approximation.

We can note that the same features apply to the Eulerian description, except that instead of the larger-scale density contrast the key quantity is the larger-scale velocity. Then, it happens that CDM power spectra are fully within the range where the velocity integral analogous to Eq.(82) converges.

V. DISCUSSIONS

We have applied to the Lagrangian formalism a resummation scheme developed in [13] within the Eulerian description. This is based on the resummation of a certain type of diagrams, called "principal-path diagrams" in [13], that may be expected to dominate the dynamics in a high-k limit. In the Eulerian case, these diagrams can be explicitly computed, order by order, and resummed, as one can recognize the exponential function in the series expansion obtained in this manner. This leads to a Gaussian decay of the form $e^{-e^{2\eta}k^2\sigma_v^2/2}$ at high k.

It is more difficult to apply the same method to the Lagrangian formalism, as the diagrams have a slightly more intricate expression and one cannot identify from the series a well-known mathematical function. However, as shown in [16], it is possible to identify this resummation with the solution of an effective linear dynamics. Then, instead of computing explicitly all diagrams and next resumming their contributions (which amounts to solve for this effective equation of motion as a perturbative series), one can directly solve for this simpler dynamics. In this article, we have applied this technique to the Lagrangian description. We have shown that it is very powerful as it can be used even when no explicit analytical solutions can be found (but one can still solve numerically the relevant differential equations). Moreover, even in such cases, it is possible to obtain the exact exponents (as defined by this partial resummation) of the late-time regime, by looking for the asymptotic modes of the linear differential equations. Then, we have found a late-time power-law behavior for the propagator, which actually simply follows the linear growth e^{η} albeit with a "renormalized" amplitude slightly smaller than unity. This is quite different from the Gaussian decay obtained in the Eulerian case.

For comparison, let us briefly recall how this method applies to the Eulerian case [16]. In this case, the solution to the effective linear dynamics can be derived explicitly and it reads as

$$\delta(\mathbf{k},\eta) = e^{\eta}\delta_0(\mathbf{k})e^{e^{\eta}\hat{\alpha}_E(\mathbf{k})}, \tag{90}$$

with

$$\hat{\alpha}_E(\mathbf{k}) = \int \mathrm{d}^n\mathbf{w}\frac{\mathbf{k}.\mathbf{w}}{w^2}\delta_0(\mathbf{w}), \tag{91}$$

(using notations that straightforwardly extend those used throughout the paper). For Gaussian initial conditions the ensemble average of this expression can be easily computed. It leads to the following propagator,

$$G_E(k,\eta) = e^{\eta}\, e^{e^{2\eta}\langle\hat{\alpha}_E(\mathbf{k})^2\rangle/2}. \tag{92}$$

Because of the $\mathbf{k}$-dependence of $\hat{\alpha}_E(\mathbf{k})$, one obtains a Gaussian damping of the form $e^{-e^{2\eta}k^2\sigma_v^2/2}$ at high k, with $\sigma_v^2 = 1/n\int(\mathrm{d}^n\mathbf{w}/w^2)P_0(w)$ (n is here the number of space dimensions). As discussed above and shown in details in previous sections, our calculations in Lagrangian space do not give a closed form for the propagator but allow nonetheless to describe its properties exhaustively.

Eulerian and Lagrangian calculations prove to lead to quantitatively very different results. Whereas the decay found for the Eulerian case exhibits a Gaussian tail with a strong k-dependence, in Lagrangian variables the propagators are essentially k-independent with no significant decay at late time. After a stage of accelerated growth, followed by a transitory slow-down, the high-k modes growth is indeed found to be simply slightly retarded and still growing as e^{η} as the linear growth rate. The situation is the same in 2D and 3D cases. The delay is only slightly less important for the 3D case. The independence on wavenumber k in the Lagrangian case directly follows from the fact that the kernels α and β of Eqs.(33)-(34), that appear in the 2D equations of motion (32) and (39), are homogeneous functions of their two arguments $\mathbf{k}_1$ and $\mathbf{k}_2$: they only depend on relative angles. This also holds for the 3D dynamics, as can be checked in Eqs.(65)-(67). Therefore, this property is not restricted to the partial resummation associated with "principal-path" diagrams. In a similar fashion, the dependence on k obtained in the Eulerian case is due to the non-homogeneous character of the kernels α and β that appear in this framework, which can also be seen in Eq.(91).

As seen in the previous sections, another distinctive feature of the Lagrangian description is the important role played by parity symmetries. Indeed, whereas in the Eulerian framework the two quantities of interest, the density and the velocity divergence, are true scalars, in the Lagrangian framework we must take into account both curl-free and rotational parts of the displacement field (in Lagrangian space $\mathbf{q}$), as a curl-free Eulerian velocity field does not translate into a Lagrangian curl-free displacement field beyond second order. We have shown that keeping track of the vorticity degrees of freedom is necessary to obtain a well-defined propagator in the nonlinear regime.

How to reconcile these results? Although Eulerian and Lagrangian descriptions are ultimately equivalent, the objects we have computed are clearly distinct. In the nonlinear regime modes in Lagrangian space cannot be directly mapped to those in Eulerian space. One should then not be too surprised to find quantitatively different results. What we have computed here is in essence the leading effect of a random background on the growth of structures, assuming scales can be well separated (e.g. that the wavelength of the background modes are much larger than the modes of interest). It turns out that the Eulerian modes are sensitive to the large-scale displacement field at leading order, whereas the Lagrangian modes are not. These large-scale displacement fields are responsible for the decay of the Eulerian correlators at large time separations. Indeed, the modes behave as if they were randomly advected by the large-scale displacements [13, 16]. Basically, everything happens as if small-scale structures were moved around; and because they occupy a different location in real space, their correlation with the initial field decay. In Lagrangian space, modes are not affected by such displacements (by construction, the convergence κ and the vorticity ω are not sensitive to a uniform translation, being related to derivatives of the displacement field taken as a function of the initial conditions). They are more directly sensitive to the density field. Thus, as discussed in section IV, whereas the Eulerian propagator is governed by the amplitude of the larger-scale velocity, the Lagrangian propagator is governed by the amplitude of the larger-scale density. Then, the leading effect resembles more a tidal effect. What we have found is that modes are not disrupted by the accumulation of those tidal effects, at this order of the calculation, e.g., the results displayed in Figs. 3 and 4 suggest that there is no true loss of memory nor efficient relaxation associated with the gravitational dynamics. It is not clear then how this loss of memory - which is expected to happen eventually in the nonlinear regime - could take place. Whether it can be described with the help of additional diagrams[23], from terms beyond the high-k limit; or whether we have to go beyond shell-crossing (which breaks the analyticity of the Jacobian) to capture possible relaxation effects, is yet unclear.

Acknowledgments

It is a pleasure to thank Román Scoccimarro and Martín Crocce for fruitful discussions and suggestions. This work was supported in part by the French Programme National de Cosmology and by the French Agence National de la Recherche under grant BLAN07-1-212615.

APPENDIX A: ALTERNATIVE EQUATIONS FOR THE 2D DYNAMICS

Here we explore in a more details the properties of system (47)-(48). With the change of variable $D = e^{\eta}$ it yields,

$$D^2 \frac{\mathrm{d}^2\hat{\kappa}}{\mathrm{d}D^2} + \frac{7}{2} D \frac{\mathrm{d}\hat{\kappa}}{\mathrm{d}D} \; = \; \hat{\alpha} D \left[D^2 \frac{\mathrm{d}^2\hat{\kappa}}{\mathrm{d}D^2} + \frac{7}{2} D \frac{\mathrm{d}\hat{\kappa}}{\mathrm{d}D} + \frac{3}{2}\hat{\kappa} \right] + \hat{\beta} D \left[D^2 \frac{\mathrm{d}^2\hat{\omega}}{\mathrm{d}D^2} + \frac{7}{2} D \frac{\mathrm{d}\hat{\omega}}{\mathrm{d}D} + \frac{3}{2}\hat{\omega} \right] \quad \text{(A1)}$$

$$D \frac{\mathrm{d}\hat{\omega}}{\mathrm{d}D} + \hat{\omega} \; = \; -\hat{\beta} D^2 \frac{\mathrm{d}\hat{\kappa}}{\mathrm{d}D} + \hat{\alpha} D^2 \frac{\mathrm{d}\hat{\omega}}{\mathrm{d}D} \quad \text{(A2)}$$

with the initial conditions:

$$D \to 0: \quad \hat{\kappa} = 1 + \frac{3}{7}\hat{\alpha} D, \quad \hat{\omega} = 0. \quad \text{(A3)}$$

Equation (A1) can be integrated once to give:

$$D \frac{\mathrm{d}\hat{\kappa}}{\mathrm{d}D} + \frac{5}{2}\hat{\kappa} - \frac{5}{2} = \hat{\alpha} D \left[D \frac{\mathrm{d}\hat{\kappa}}{\mathrm{d}D} + \frac{3}{2}\hat{\kappa} \right] + \hat{\beta} D \left[D \frac{\mathrm{d}\hat{\omega}}{\mathrm{d}D} + \frac{3}{2}\hat{\omega} \right] \quad \text{(A4)}$$

Then, eliminating $\hat{\omega}$ from Eqs.(A2)-(A4) gives the second-order equation for $\hat{\kappa}$:

$$2(1-3\hat{\alpha}D) D^2 \frac{\mathrm{d}^2\hat{\kappa}}{\mathrm{d}D^2} + (7-15\hat{\alpha}D) D \frac{\mathrm{d}\hat{\kappa}}{\mathrm{d}D} + \frac{\hat{\alpha}D(1-\hat{\alpha}D)}{(1-\hat{\alpha}D)^2 + (\hat{\beta}D)^2} [12\hat{\kappa} - 15] = 0 \quad \text{(A5)}$$

We can note that for $\hat{\beta} = 0$ the divergent part $\hat{\kappa}$ decouples from the vorticity $\hat{\omega}$ and the solution of Eq.(A1) can be written as

$$\hat{\kappa}(D; \hat{\alpha}, 0) = {}_2F_1(1, 3/2; 7/2; \hat{\alpha} D). \quad \text{(A6)}$$

It exhibits a singularity at the point $D = 1/\hat{\alpha}$ (for $\hat{\alpha} > 0$), in agreement with Eq.(61), but it actually remains finite at this point and has a well-behaved analytic continuation beyond, as seen in Fig. 5.

Here we can note that writing the high-k resummation in terms of the differential equations (44)-(45), and the propagator with the integral representation (55), is a key ingredient to obtain the asymptotic behaviors. Indeed, computing $G(k,\eta)$ from its diagrammatic expansion, which amounts to expand the integrand in Eq.(55) over powers of $\hat{\alpha}$ and $\hat{\beta}$, leads to an asymptotic series with zero radius of convergence. For instance, for $\hat{\beta} = 0$ we directly obtain from Eq.(A6)

$$\hat{\kappa}(D; \hat{\alpha}, 0) = \sum_{p=0}^{\infty} \frac{15}{(2p+3)(2p+5)} \hat{\alpha}^p D^p, \quad \text{(A7)}$$

which gives after we average over $\hat{\alpha}$:

$$\langle \hat{\kappa}(D; \hat{\alpha}, 0) \rangle_{\hat{\alpha}} = \sum_{p=0}^{\infty} \frac{15\,(2p-1)!!}{(4p+3)(4p+5)} (3\sigma_2^2)^{2p} D^{2p}. \quad \text{(A8)}$$

This asymptotic series describes the early rise of $\hat{G}$ but it cannot give (without ambiguities) the late-time relaxation to a constant.

This behavior emerges because of the existence of the second degree of freedom associated with the vorticity, $\hat{\beta}$. To take it into account, one may look for a solution of Eqs.(A2)-(A4) as a perturbative series over powers of D, as in Eq.(A7). Then, computing the first few terms or looking at simplified cases suggests that the nonzero variance of $\hat{\beta}$ decreases somewhat the coefficients of Eq.(A8) but they remain positive and fastly growing (it typically modifies Eq.(A8) by changing the factor $(3\sigma_2^2)^{2p}$ into $(2\sigma_2^2)^{2p}$, because of Eq.(52)). Thus, as expected the vorticity slows down the rise of the propagator $G(k,\eta)$ but its magnitude is not sufficient to make it decay with respect to the linear propagator at early times. Nevertheless, it is necessary to take into account the vorticity to obtain the late-time behavior of $G(k,\eta)$.

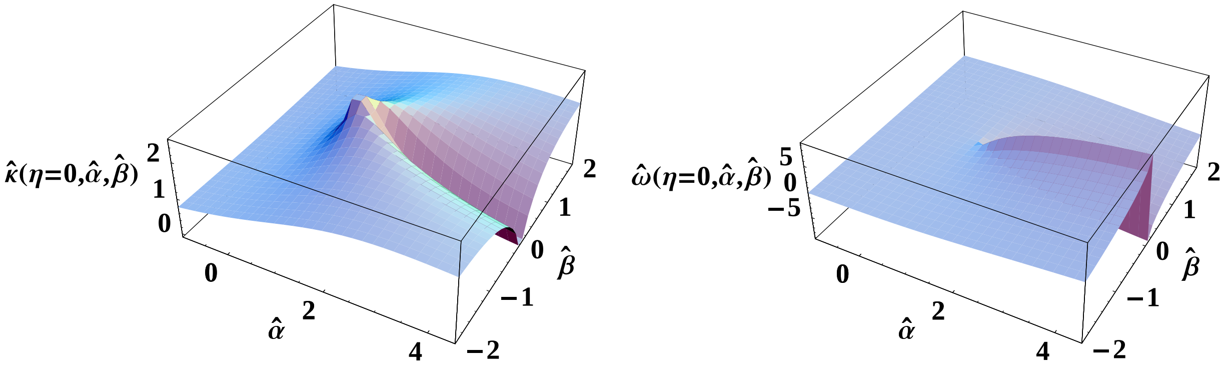

FIG. 5: The divergence $\hat\kappa(\eta = 0; \hat\alpha, \hat\beta)$ (left panel) and the vorticity (right panel) as a function of $\hat\alpha, \hat\beta$. The divergence reaches a constant at large radius, $\sqrt{\hat\alpha^2 + \hat\beta^2} \to \infty$, for a fixed polar angle. The divergence is found to be continuous and even with respect to $\hat\beta$; the vorticity is found to be discontinuous along the critical half-line $e^\eta \hat\alpha > 1$, $\hat\beta = 0$, and odd with respect to $\hat\beta$.

[1] P. J. E. Peebles, *The large-scale structure of the universe* (Research supported by the National Science Foundation. Princeton, N.J., Princeton University Press, 1980. 435 p., 1980).

[2] F. Bernardeau, S. Colombi, E. Gaztañaga, and R. Scoccimarro, *Phys. Rep.* **367**, 1 (2002).

[3] Y. B. Zel'Dovich, *Astr. & Astrophys.* **5**, 84 (1970).

[4] J. A. Peacock and S. J. Dodds, *Mon. Not. R. Astr. Soc.* **280**, L19 (1996).

[5] R. E. Smith, J. A. Peacock, A. Jenkins, S. D. M. White, C. S. Frenk, F. R. Pearce, P. A. Thomas, G. Efstathiou, and H. M. P. Couchman, *Mon. Not. R. Astr. Soc.* **341**, 1311 (2003), arXiv:astro-ph/0207664.

[6] A. J. S. Hamilton, P. Kumar, E. Lu, and A. Matthews, *Astrophys. J. Letter* **374**, L1 (1991).

[7] A. Cooray and R. Sheth, *Phys. Rep.* **372**, 1 (2002), astro-ph/0206508.

[8] M. Crocce and R. Scoccimarro, Phys. Rev. D **73**, 063519 (2006), astro-ph/0509418.

[9] P. Valageas, *Astr. & Astrophys.* **465**, 725 (2007), arXiv:astro-ph/0611849.

[10] S. Matarrese and M. Pietroni, ArXiv Astrophysics e-prints (2007), astro-ph/0703563.

[11] P. McDonald, Phys. Rev. D **75**, 043514 (2007), arXiv:astro-ph/0606028.

[12] P. Valageas, ArXiv e-prints **711** (2007), 0711.3407.

[13] M. Crocce and R. Scoccimarro, Phys. Rev. D **73**, 063520 (2006), astro-ph/0509419.

[14] M. Crocce and R. Scoccimarro, ArXiv e-prints **704** (2007), 0704.2783.

[15] T. Matsubara, ArXiv e-prints **711** (2007), 0711.2521.

[16] P. Valageas, *Astr. & Astrophys.* **476**, 31 (2007), arXiv/0706.2593.

[17] C. Pichon and F. Bernardeau, *Astr. & Astrophys.* **343**, 663 (1999), arXiv:astro-ph/9902142.

[18] F. Bernardeau, Astrophys. J. **427**, 51 (1994), arXiv:astro-ph/9311066.

[19] F. Bernardeau, *Cosmologie, des fondements théoriques aux observations* (Editions du CNRS et EDP Sciences, 2007).

[20] P. Valageas, *Astr. & Astrophys.* **421**, 23 (2004), arXiv:astro-ph/0307008.

[21] Although these equations appear to be of different order they are equivalent at least as long as the transform from $\mathbf{x}$ to $\mathbf{q}$ is regular, i.e. before shell crossings. In 2D, both equations lead to the same constraint equation. In 3D they lead to different sets of three equations that have the form of systems of linear equations in $\partial\psi'_i/\partial q_j$ ($\partial\psi_i/\partial q_j$ being treated as parameters). As such, one system can be transformed into the other by linear transforms.

[22] The propagator can also be obtained as the ensemble average of the product of $\kappa(\mathbf{k},\eta)$ and $\kappa_0(\mathbf{k}')$, $\langle\kappa(\mathbf{k},\eta)\kappa_0(\mathbf{k}')\rangle = \delta_{\rm D}(\mathbf{k}-\mathbf{k}')G(k,\eta)P_0(k)$. As shown in [8] the two quantities are identical for Gaussian initial conditions.

[23] We can note that including other diagrams would mean that the incoming waves are not necessarily in the linear regime. They would then have not only different statistical properties but also different time dependences.